

thought to arise from the cyclized carbon attached to the exocyclic methylene (carbon 8). The peaks resonating at 127ppm and 138ppm in the spectrum of the Yallourn resinite have been assigned to the protonated (carbon 12) and quaternary (carbon 13) carbons of the side chain double bond by chemical shift comparisons with model compounds (27-28) and by previously reported dipolar dephasing experiments (12). Relative peak areas for each resonance in the olefinic region as well as the total olefinic carbon content of the spectra indicate that the total olefinic content, in a 20 carbon structural unit, progressively decreases from approximately 4 carbons per monomer in the spectrum of the Yallourn resinite to approximately 2 carbons per monomer in the spectrum of the Brunner resinite. As the thermal maturation of the resinite increases, there is a decrease of nearly 50% for the olefinic carbons in the samples being studied. This loss corresponds to the transformation of diterpenoids containing two double bonds (polycommunic acid units) to diterpenoids having only one double bond.

Integration of the carboxylic acid resonances, peaks at 186ppm and 181ppm, of the spectra of the Yallourn and Morwell resinites and 186ppm, 181ppm and 177ppm for the spectrum of the Brunner resinite, yielded values of 0.8, 0.7, and 0.5 carbons per monomer, respectively. As the degree of maturation increases, there appears to be a decrease in intensity of the peaks resonating at 186ppm and 181ppm with an additional resonance in the carboxyl region centered around 177ppm visible in the spectrum of the Brunner resinite. The broad peak resonating between 201ppm and 210ppm in the spectra of the Morwell and Brunner resinites has been assigned to ketones resulting from oxidation (18).

The intramolecular cyclization of the exocyclic methylene to form a mono-unsaturated C ring (Figure 2), is entirely consistent with pyrolysis and NMR data. The positioning of the double bond between carbons 8 and 17 (of the communic acid monomer) will stabilize the B and C rings thus making cleavage of the A ring rather than the B or C rings the more likely site of pyrolysis. The compound(s) expected to dominate the pyrolysis of a polymeric tricyclic acid (as described above) are alkyl naphthalenes and alkyl hydronaphthalenes. With this information, the combined results of the quantitative NMR data and py/gc/ms data, it is possible to rule out proposed mechanisms of maturation other than that of intramolecular cyclization which appears to correlate with all the chemical data.

#### SESQUITERPENOID-TYPE RESINITES

The general consensus regarding the structure of sesquiterpenoid resinites is that the maceral exists as two fractions. One fraction consists of a high molecular weight (HMW) polymer proposed to be that of polycadinene (PC)(30) and the second fraction is composed of low molecular weight compounds shown by gas chromatography/ mass spectrometry (GC/MS) to be dimers and trimers of cadinene and functionalized triterpenoids (30-32).

In this report, we will discuss the results of a series of experiments which were carried out in an effort to characterize the polymeric fraction of an immature resin, a precursor to sesquiterpenoid-based resinites. By examining the structure of polycadinene from a young resin such as a Dammar resin, we would be able to compare these structural characteristics with those of more mature resinites such as that described from the Blind Canyon coal (33-34). From this comparison the chemical changes that accompany the maturation process can be identified thus further aiding in the structural identification of the Blind Canyon coal's resinite maceral.

The Dammar resin was chosen due to its availability in a relatively pure form. In addition, this particular resin is extremely soluble in  $\text{CDCl}_3$ . Solubility in  $\text{CDCl}_3$  was an important consideration, since NMR was chosen as the primary structural tool for this study. NMR techniques, which include one- and two-dimensional NMR spectra, were used in this study to determine the consistency of the structure of a high molecular weight methanol insoluble fraction of the Dammar resin (the polycadinene biopolymer as suggested by van Aarssen et al.(30)) with that of a theoretical polycadinene polymer and to propose possible chemical alterations induced during catagenesis.

The resin selected for this study is a commercially available Dammar resin purchased from Aldrich Chemical Co. The Dammar resin was first dissolved in 50 mL of hexane then approximately 5 mL of methanol was added to precipitate the polymer as a white powder following the procedure described by van Aarssen et. al. (30). The powder was then separated by centrifugation and washed with methanol. The methanol was evaporated and replaced with approximately 0.6 mL of  $\text{CDCl}_3$ , a solvent suitable for NMR spectroscopy.

The high resolution liquid  $^1\text{H}$  and  $^{13}\text{C}$  NMR experiments were performed on a Bruker AMX-360 spectrometer equipped with a 5mm inverse-detected probe. The one-dimensional single pulse  $^1\text{H}$  and  $^{13}\text{C}$  experiments were carried out using a  $30^\circ$  flip angle. The  $^{13}\text{C}$  distortionless polarization transfer (DEPT) experiments were carried out using  $45^\circ$  (3.3  $\mu\text{s}$ ),  $90^\circ$  (6.6  $\mu\text{s}$ ), and  $135^\circ$  (16.5  $\mu\text{s}$ )  $^{13}\text{C}$  read pulses, respectively. A solid state  $^{13}\text{C}$  CPMAS spectrum was obtained on a Chemagnetics M-100 NMR spectrometer. The pertinent parameters are found elsewhere (33). A two-dimensional high resolution liquid experiment COSY (homonuclear correlation) with a  $45^\circ$

read pulse was performed on the HMW fraction isolated from the Dammar resin using a standard Bruker experiment.

Elemental analyses of the methanol insoluble fraction of the extant Dammar resin as well as previously reported data for resinite from the Blind Canyon coal can be seen in Table 1. Included in Table 1 are the calculated oxygen and hydrogen weight percentages of a pure polycadinene polymer (structure shown in Figure 4), which has the monomeric formula  $C_{15}H_{26}$ , and the monomeric formula of the HMW Dammar polymer. It can be inferred from this table that the polymeric constituent of the Dammar resin does not differ significantly from that of the Blind Canyon resinite. Also evident in this table are the considerable differences between the polymer isolated from the extant Dammar resin and that of a pure polymer composed solely of cadinene monomers. The Dammar PC elemental data suggests the presence of approximately one oxygen atom for every two cadinene monomers (assuming 15 carbons per monomer) and two less hydrogen atoms than the cadinene's 26.

$^{13}C$  NMR was used to identify the functional groups and substitution patterns of the carbons present in the polycadinene fraction of the Dammar resin. Figure 5a-d shows high resolution  $^{13}C$  NMR spectra of the polycadinene from Dammar resin in  $CDCl_3$ . Figure 5a is a quantitative decoupled  $^{13}C$  NMR spectrum, while Figures 5b-d are the  $^{13}C$  distortionless polarization transfer (DEPT) used to aid in assigning carbon substitution. The aliphatic region of the spectrum (0 ppm to 60 ppm) is extremely complex and contains a number of sharp signals far greater than what can be anticipated for pure polycadinene. The olefinic region of the spectrum (120 ppm to 140 ppm) is not as complex, however, but it is still not consistent with the structure of a pure cadinene monomer. In cadinene, there are two olefinic carbons with one being a tertiary carbon and the other a quaternary carbon. The spectrum shows at least four peaks.

The spectra shown in Figures 5b-d are the three  $^{13}C$  DEPT experiments ( $45^\circ$ ,  $90^\circ$ , and  $135^\circ$ ). From these spectra and the spectrum in Figure 5a, the functional group assignments can be made. Chemical shift analysis of the spectrum in Figure 5a is used as a preliminary means of assigning carbon substitution, while the DEPT spectra provide a means of sorting or spectrally editing the signals. For example, the DEPT  $45^\circ$  spectrum contains  $CH_3$ ,  $CH_2$ , and  $CH$  carbons with the most intense signals emanating from the  $CH_2$  carbons. The DEPT  $90^\circ$  spectrum contains only  $CH$  carbons, and the DEPT  $135^\circ$  spectrum contains positive signals from the  $CH$  and  $CH_3$  carbons, but negative signals from the  $CH_2$  carbons. Thus when the results from the three DEPT spectra are combined all the protonated carbons can be assigned. The non protonated carbons are assigned by difference from the  $^{13}C$  broadband decoupled spectrum.

To further aid in the structural elucidation of the Dammar HMW resin polymer, two dimensional (2D) NMR data was obtained. 2D-NMR is capable of correlating and spreading out NMR spectral data thus providing a means of confirming one dimensional spectral assignments while at the same time providing structural information concerning molecular connectivity. The 1H-1H correlation spectrum (COSY) for the HMW fraction of the Dammar resin is shown in Figure 6. From the two dimensional NMR spectrum it is possible to determine the association of protons in the one dimensional spectrum.

It is clear from the detailed NMR studies presented here that the HMW polymer isolated from Dammar resin is not purely polycadinene. By examination of the olefinic region, we observe at least four peaks indicating four different environments where only two would be expected in a pure polymer of polycadinene. Integration of these peaks indicates that approximately 1.5 olefins are present per 15-carbon unit, and we would expect 2 such carbons in the pure polymer. The aliphatic region contains many more peaks than would be expected for pure polycadinene. These results suggest that the polymer from Dammar resin is not represented by a pure polycadinene structure. We suggest that the general structural makeup of the polymer is similar to the polycadinene structure but that only two of three units contain olefinic carbons, the other is fully saturated. In addition, on average the olefinic carbons in two units containing such carbons are not at the same site in the structure. This would account for four peaks being present in the NMR spectra. The structure shown in Figure 4 depicts our model for polycadinene structures which comprise sesquiterpenoid resins.

## References

1. Dyrkacz, G. R., Horwitz, E. P., *Fuel*, **61**, 3, 1982.
2. Dyrkacz, G. R., Bloomquist, C. A. A., and Ruscio, L., *Fuel*, **63**, 1367, 1984.
3. Greenwood, P. F., Zhang, E., Vastola, F. J. and Hatcher, P. G., *Anal. Chem.*, **65**, 1937, 1993.
4. Stout, S. A. and Hall, K. J., *J. Anal. Appl. Pyrol.*, **21**, 195, 1990

- 5 Stout, S. A., Boon, J. J. and Spackman, W., *Geochim. Cosmochim. Acta*, **52**, 405, 1988.
- 6 Hatcher, P. G., *Organic Geochemistry*, **16**, 959, 1990.
- 7 Faulon, J. L. and Hatcher, P. G., *Energy & Fuels* (in press).
- 8 Hatcher, P. G., Wenzel, K. A. and Faulon, J.-L., Preprints, American Chemical Society Fuel Division, **38**, 1270, 1993.
- 9 Langenheim, J. H. *Science*, **163**, 1157, 1969.
- 10 Brooks, J. D. and Stevens, J. R., *Fuel*, **46**, 13, 1967.
- 11 Cunningham A., Gay, I. D., Oechslinger, A. C., and Langenheim, J. H., *Phytochem*, **22(4)**, 965, 1983.
- 12 Wilson, M. A., Collin, P. J., Vassallo, A. M., and Russel, N. J., *Org. Geochem.*, **7(2)**, 161, 1984.
- 13 Anderson, K. A., Botto, R. E., Dyrkacz, G. R., Hayatsu R., and Winans, R. E., *Fuel*, **69**, 934, 1990.
- 14 Thomas, B. R., *Organic Geochemistry - Methods and Results*, Springer-Verlag, 599-618, 1969.
- 15 Carman, R. M., Cowley, D. E., and Marty, R. A., *Aust. J. Chem.*, **23**, 1655, 1970.
- 16 Beck, C. W., *Appl. Spec. Rev.*, **22(1)**, 57, 1986.
- 17 Vassallo, A. M., Liu, Y. L., Pang, L. S. K., and Wilson, M. A., *Fuel*, **70**, 635, 1991.
- 18 Wilson, M. A., Hanna J. V., Cole-Clarke, P. A., Greenwood, P. F., and Willett, G. D., *Fuel*, **71**, 1097, 1992.
- 19 Wilson, M. A., Hanna J. V., Cole-Clarke, P. A., Willett G. D., and Greenwood, P. F., *Org. Geochem.*, **18(4)**, 555, 1992.
- 20 Anderson, K. B., Winans R. E., and Botto R. E., *Org. Geochem.*, **18(6)**, 829, 1992.
- 21 Challinor, J. M., *J. Anal. Appl. Pyrol.*, **16**, 323, 1989.
- 22 Nobes, E. D., *Trans. R. Soc. South Aust.*, **46**, 528, 1992.
- 23 Suggate, R. P., *N.Z.J. Sci. Technol.*, **B31(4)**, 1, 1950.
- 24 Grimalt J. O., Simoncit, B. R. T., Hatcher, P. G., and Nissenbaum A., *Org. Geochem.*, **13**, 677, 1988.
- 25 van Aarssen, B. K. G., and Deleeuw, J. W., *Am. Chem. Soc. Div. Fuel Chem. Prepr.*, **36(2)**, 774, 1991.
- 26 van Aarssen, B. K. G., and Deleeuw, J. W., *Geochem. Cosmochim. Acta.*, submitted for publication, 1992.
- 27 Clifford, D. J., and Hatcher, P. G., *Org. Geochem.*, submitted for publication, 1993.
- 28 Wenkert, E., and Buckwalter, B. L., *J. Am. Chem. Soc.*, **94(12)**, 4367, 1972.
- 29 Lambert, J. B., and Frye, J. S., *Science*, **217**, 55, 1982.
- 30 van Aarssen, B. G. K., Cox, H. C., Hoogendoorn, P., and de Leeuw, J. W., *Geochem. Cosmochim. Acta.*, **54**, 3021, 1991.
- 31 Crelling, J. C., Pugmire, R. J., Meuzelaar, H. L. C., McClennen, W. H., Huai, H. and Daras, J., *Energy & Fuels*, **5**, 688, 1991.
- 32 Meuzelaar, H. L. C., Huai, H., Lo, R. and Dworzanski, J. P., *Fuel Proc. Technol.*, **28**, 119, 1991.
- 33 Clifford, D. J., Hou, L., Bortiatynski, J. M. and Hatcher, P. G., Technical Progress Report February - 1993, Prepared for the U.S. DOE under Contract No. DE-FG22-92PC92104.
- 34 Hou L., Clifford, D. J., Bortiatynski, J. M., and Hatcher, P. G., Technical Progress Report October - 1993, Prepared for the U.S. DOE under Contract No. DE-FG22-92PC92104.

Table 1. Ultimate analysis (DMMF) of the HMW fraction from a Dammar resin, the resinite from a Blind Canyon coal sample, and pure polycadinene.

Sample	% C	% H	% O	Monomeric Formula
HMW polymer (Dammar)	84.2	11	4.8	C <sub>15</sub> H <sub>24</sub> O <sub>0.65</sub>
Whole resinite (DECS16)	86.2	10.4	3.4	
Polycadinene (pure polymer)	87.3	12.7	0	C <sub>15</sub> H <sub>26</sub>

\* Obtained by difference.

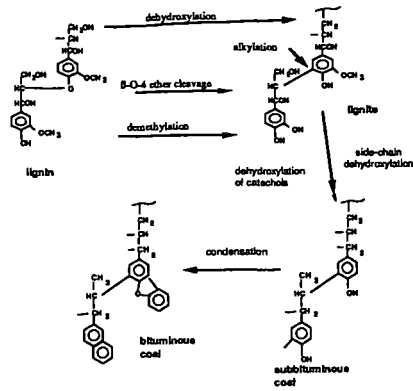


Figure 1. Sequence of reactions proposed for the coalification of lignin in wood to coalified wood of the rank of bituminous coal.

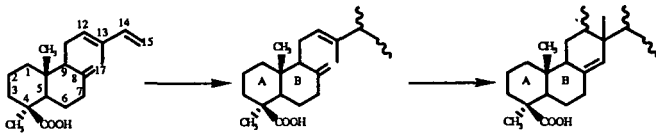


Figure 2: Polymerization of communic acid to *trans*-14,15-polycommunic acid followed by the intramolecular cyclization of carbons 17 and 13.

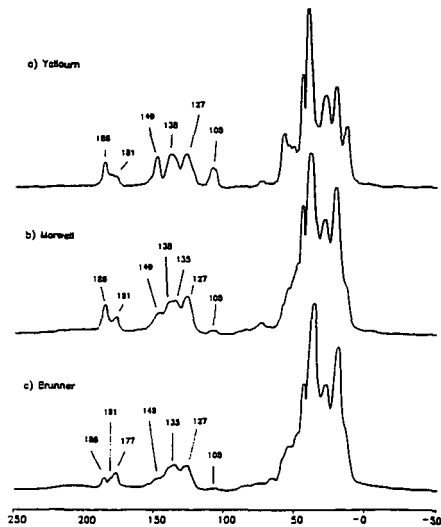


Figure 3: <sup>13</sup>C CPMAS NMR of diterpenoid resinites.

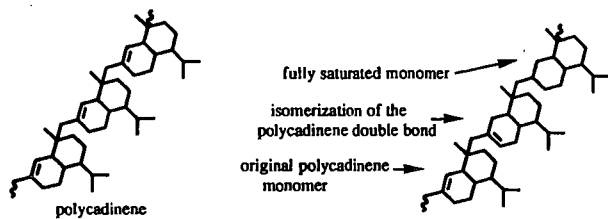


Figure 4: Polycadinene polymer and polymer containing possible transformations of the cadinene monomers.

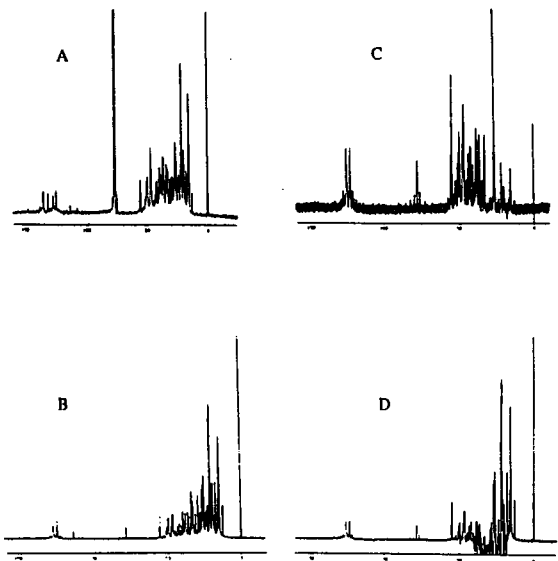


Figure 5:  $^{13}\text{C}$  broadband decoupled (A),  $45^\circ$  DEPT (B),  $90^\circ$  DEPT (C), and  $135^\circ$  DEPT (D) NMR spectra of HMW fraction of Dammar resin in  $\text{CDCl}_3$ .

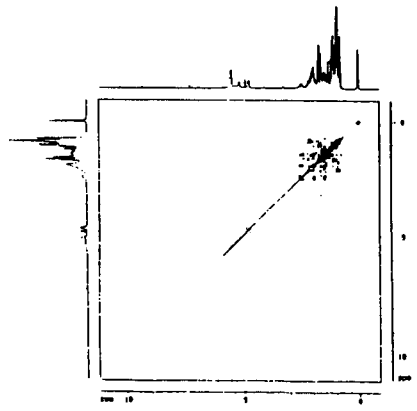


Figure 6:  $^1\text{H}$ - $^1\text{H}$  correlation spectrum (COSY  $45^\circ$ ) of the high molecular weight fraction of the Dammar resin in  $\text{CDCl}_3$ .

# Scanning Transmission X-ray Microscopy: A New "Looking Glass" into Coal Chemical Structure

Robert E. Botto and George D. Cody

Chemistry Division, Argonne National Laboratory, 9700 So. Cass Ave.  
Argonne, IL 60439

Keywords: Microscopy, X-ray, Coal

## Introduction

Since the early observations by Thiessen<sup>1</sup> and later by Stach,<sup>2</sup> who first recognized coal to be an extremely heterogeneous substance having distinguishable components that could be readily observed only with a microscope, the discipline of coal petrography has had enormous impact on the entire field of coal science. Following the realization that coal is composed of widely diverse, yet totally recognizable fossilized plant materials that have been converted into one or more macerals during coalification, coal chemists began to study the isolated maceral constituents individually. Characterization of their properties revealed that these individual constituents had chemistries as rich and diverse as the mosaic textures that had been seen for macerals microscopically, and as a result, a new level of understanding of the chemistry of coal has been attained.

Notwithstanding the enormous strides that have been made in the chemical characterization of macerals, facilitated primarily by the aid of elegant separation methods,<sup>3</sup> there has been no direct correlation of the optical textures observed under a microscope with maceral chemistry. Moreover, an important issue still to be resolved is whether the macerals themselves are chemically homogeneous or whether there is heterogeneity on a still smaller scale.

In this paper we report, for the first time, the use of scanning transmission x-ray microscopy (STXM) to spatially map the chemistry of aromatic and aliphatic carbon functionalities in coal to a resolution of less than 0.1  $\mu\text{m}$ . In addition, localized x-ray absorption spectroscopy recorded at the carbon K absorption edge have facilitated analysis of the variations in fundamental chemistry at maceral interfaces and within maceral boundaries.

## Results and Discussion

Measurements were performed at the National Synchrotron Light Source at Brookhaven National Laboratory using the soft x-ray microscope facility (line X1A).<sup>4,5</sup> The wavelength of the x-ray beam was selected by a spherical-grating monochromator having a bandwidth of 6 pm for a 180- $\mu\text{m}$  exit slit; this corresponds to an energy band width of 0.7 eV at a photon energy of about 290 eV. The specimens were mechanically scanned under computer control, and transmitted x-rays were detected by a gas flow counter. The microscope was enclosed in a helium atmosphere and was separated from the beamline vacuum by a 120-nm silicon nitride membrane. Coal specimens were ultramicrotomed to a thickness of approximately 200 nm for analysis.

Images of three distinct regions within a microtomed thin section of hvA Pittsburgh bituminous coal (APCS No. 4) recorded at photon energies of 285.5 eV (left column) and 288.1 eV (right column) are shown in Figure 1. Chemical contrast can clearly be discerned between image pairs taken at the two energies, and this chemical specificity can be related to differences in x-ray absorption near-edge structure (XANES) cross sections of  $\text{sp}^2$ - and  $\text{sp}^3$ -carbon functional groups. Other features seen in the images may be due to variations in sample thickness or to regions of matter with different densities; however, these can easily be distinguished from chemical variations by the lack of contrast reversal between image pairs.

Two fundamental types of features can be readily distinguished within the top pair of micrographs shown in Figure 1. The narrow feature running from the top left to lower right portion of the image exhibits high absorptivity at 288.1 eV ( $\text{sp}^3$ -absorption band) and correspondingly little absorptivity at 285.5 eV ( $\text{sp}^2$ -absorption band). This response is typical of highly aliphatic material, and taken together with the morphology of this feature, suggests that it may be the maceral cutinite embedded within a more highly aromatic, or vitrinite, matrix. The diagonal stripes that traverse the image in the opposite direction show no contrast reversal, hence are likely to be scoring marks made by the microtome blade.

The middle two micrographs contain structures that exhibit somewhat different behavior. Two large elliptical bodies are evident which show lower absorptivity in the 285.5 eV image than the surrounding material; however, very little image contrast is observed at an energy of 288.1 eV. The contrast seen in the image recorded at the  $\text{sp}^2$  absorption energy suggests that the elliptical bodies contain more highly aliphatic material than the surrounding regions, and given this difference in chemistry, lack of contrast in the  $\text{sp}^3$  image implies that these domains contain less dense material as well. The morphology and chemistry suggests that these elliptical regions are microspores. Within the upper microspore, a small x-ray

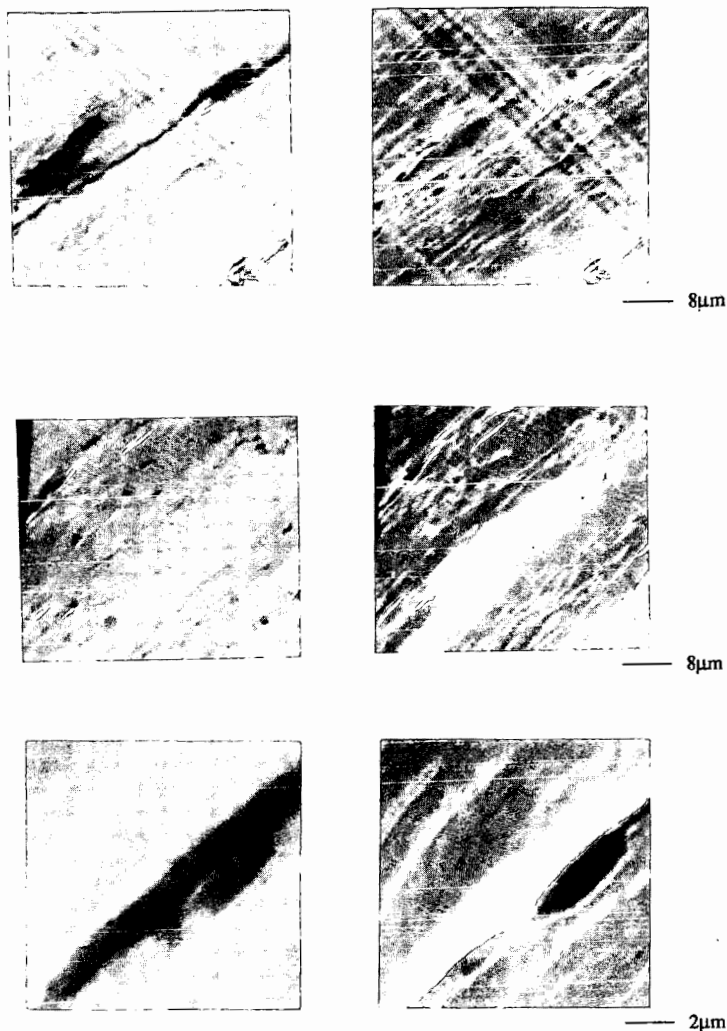


**Figure 1.** Scanning transmission x-ray micrographs of three regions within a 200-nm microtomed section of hvA Pittsburgh bituminous coal (APCS No. 4) recorded at photon energies of 285.5 eV ( $sp^2$  absorption) and 288.1 eV ( $sp^3$  absorption) at the carbon K-edge.

transparent region is observed whose  $sp^3$ -absorption image contrast is reversed, clearly demonstrating intramaceral heterogeneity. Other aliphatic structures are also observed in the lower portion of the micrograph. The morphology of the thin sinuous feature at the lower right is suggestive of the maceral, cutinite. Bright features clearly visible at both energies are cracks which formed as a result of microtoming the sample.

The lower two micrographs represent an expanded view of a cutinite band similar to that represented in the first images above. The cusp found near the center provides additional support for the assignment that this maceral is cutinite. The dark pod that appears at the right of the cutinite band exhibits high absorptivity at both energies; upon careful inspection, several similar structures may be identified in the top pair of micrographs as well.

In order to elucidate the chemistry of the features seen in the lower micrographs, microfocus XANES spectra were taken at various points within individual structures. Figure 2 shows XANES spectra that were taken within regions of the cutinite band, the dark pod and surrounding vitrinite. It should be noted that the spectra are not totally quantitative, especially at the higher energies, due to high absorptivity of the specimens. These effects

also limit chemical contrast in images taken at the higher energy. The cutinite spectrum exhibits a strong absorption at 288.1 eV and a relatively weak absorption centered at 285.5 eV, which is consistent with its aliphatic nature. On the other hand, XANES spectra of the dark pod and surrounding vitrinite show intense  $sp^2$  absorptions. The relative intensity ratios between  $sp^2$ - and  $sp^3$ - absorption bands in both spectra are also remarkably similar. This implies that the unknown pod structure must be composed of a denser material but is similar in chemical composition to the surrounding vitrinite.

Reflected light microscopic (ROM) analysis of the same sample using standard immersion oil techniques lends support to the assignment of vitrinite, cutinite, and microspores by STXM. Vitrinite and cutinite macerals are abundant in this coal; however, the assignment of microspores is somewhat more tenuous. ROM reveals some microspore structures having elliptical cross-sections with dimensions in the micron range. Moreover, no other potential candidates in this size range and with these morphologies were observed. Consequently, the assignment of microspores to the aliphatic entities shown in the middle micrographs is certainly reasonable.

The ability of STXM to map the chemical composition to this resolution has provided rich detail into the chemical and physical heterogeneity of a coal (APCS No. 4) regarded as being reasonably homogeneous, i.e., containing about 85% vitrinite. However, the variety of textures seen are not limited to those presented in this preliminary report. Vitrinite regions having subtle chemical differences, morphologically different exinite bodies, and microfine mineral particles and veins have also been observed and will be discussed. Recent studies toward the characterization of other Argonne Premium coals and results extending present capabilities to include STXM at the oxygen and calcium K-absorption edges will also be discussed.

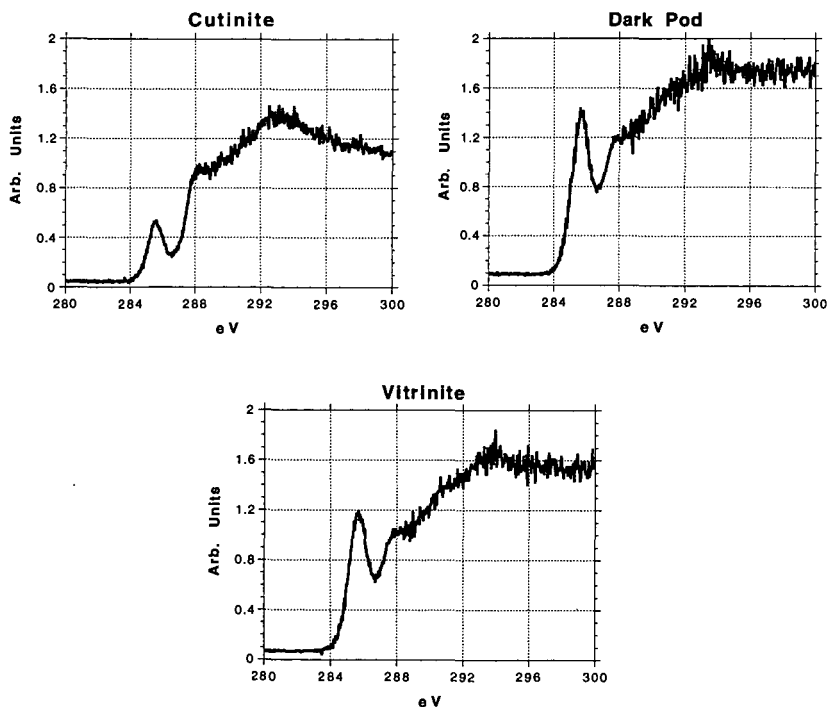


Figure 2. Carbon K-edge XANES spectra of selected regions within (A) the cutinite band, (B) the dark pod and (C) surrounding vitrinite that are identified (see text) in the lower micrographs of Figure 1.

### **Acknowledgment**

We express our gratitude to Nester J. Zaluzec and Russell E. Cook of the Materials and Components Technology Division at Argonne for their advice and help in the preparation of some of the samples, to Susan Wirick and Chris Jacobsen of the Department of Physics at SUNY Stony Brook for their help with data acquisition, conversion and transfer, and to the staff of the Coal Petrology Laboratory at Penn State University for their help with ROM. Support of this work from the Office of Basic Energy Sciences, Division of Chemical Sciences, U. S. Department of Energy is gratefully acknowledged. This work was performed at the National Synchrotron Light Source, which is supported by the Department of Energy, Office of Basic Energy Sciences.

### **References**

1. Thiessen, R. *Bur. Mines Bull.* **1920**, *117*, 296 pp.
2. Stach, E. *Lehrbuch der Kohlenpetrographie* **1935**, Borntraeger, Berlin.
3. Dyrkacz, G. R. ; Horwitz, E. P. *Fuel* **1982**, *61*, 3.
4. Kirz, J.; Ade, H.; Jacobsen C.; Ko C-H; Lindaas, S.; Williams S.; Zhang, X. *AAPPS Bull.* **1992**, *2*, 15.
5. Ade, H.; Zhang, X.; Cameron, S.; Costello, C.; Kirz, J.; Williams, S. *Science* **1992**, *258*, 972.

## TARGETING SINGLE COAL MACERALS WITH DENSITY GRADIENT CENTRIFUGATION EXPERIMENTS

John C. Crelling  
Department of Geology  
Southern Illinois University  
Carbondale, IL 62901 USA

### INTRODUCTION

Since density gradient centrifugation (DGC) techniques were introduced into coal science a little over ten years ago, continuous work has been done to separate and characterize coal macerals [1-11]. To date, good separations of the liptinite, vitrinite, and inertinite maceral groups have been reported, as have separations of individual maceral types including, sporinite, resinite, cutinite, vitrinite, pseudovitrinite, semifusinite and fusinite from coal and of alginite, sporinite, and amorphous kerogen from petroleum source rocks. Most of the separations have been verified both petrographically and chemically. Chemical analysis including chromatography and spectroscopy of these separated materials show them to have diverse bulk chemistry and chemical structures. Most recently, reactivity and combustion studies on separations of both maceral groups and single macerals have shown significant differences between them. The results of all of these studies have shown the extreme heterogeneity of coal and has improved our ability to predict the behavior of coal in any process of interest.

### TARGETING SINGLE MACERALS

To obtain separations of single coal macerals from a particular coal, coal maceral groups (liptinite, vitrinite, and inertinite) must first be concentrated. The common procedure is to do an initial two gram DGC run to obtain a density profile. Two grams is the maximum sample capacity of the standard two liter centrifuge bowl and usually provides enough material to give a useful density profile, if the macerals are well liberated. The normal procedure is to reduce the coal sample to micrometer size to get reasonable liberation and a minimum of mixed phase particles. From the density profile, two density cut-points are chosen, one at the liptinite/vitrinite boundary and one at the vitrinite/inertinite boundary as illustrated in Figure 1. While these cut-points can be determined by inspection, a superior technique is to do the determination by petrographic methods including white light and fluorescence analysis. Any cut-point determinations not verified by petrography are immediately open to question. Once the cut-points are in hand, quantities of the various maceral groups are concentrated by centrifugation at the chosen densities serially. It should be noted that for some research, the separations of these maceral groups are sufficient and further subdivision is not required. However, the results of such research must indicate that maceral groups and not single macerals were used.

When the separation of single coal macerals is desired, two gram quantities of the maceral group concentrates are again processed in a DGC run over the appropriate but limited density range, e.g. 1.00 g/mL to the liptinite/vitrinite cut-point for the liptinite maceral group. Such density profiles of the maceral groups usually reveal structure that indicates the presence of a number of single macerals such as cutinite, resinite, and sporinite in the liptinite group.

### SPECIAL TECHNIQUES FOR SEPARATING SINGLE MACERALS

There are a number of techniques that facilitate the separation of single macerals from coal. The three most useful are cryogenic treatment, demineralization, and semicontinuous centrifugation. While the usual techniques of micronization using a fluid energy mill or a jet mill will reduce the particle size of a sample to the micrometer range, some multiphase particles often persist. These can be reduced by immersing the sample in liquid nitrogen to freeze it and then rapidly thawing it out at room temperature. With this treatment, the multiphase particles tend to fracture along maceral boundaries. This process can be repeated with or without regrinding to achieve maximum liberation of the macerals.

Demineralization with HCl to eliminate carbonates and HF to eliminate silicates will both increase the yield of a DGC separation and increase the purity of a given density fraction by reducing mixed maceral/mineral phases. However, mineral sulfides

especially pyrite and mineral oxides will not be removed by this acid treatment. If any significant amounts of these minerals are present, a preliminary sink/float separation at a density of about 1.7 g/mL has been found to improve the DGC separation. In cases where pyrite is extremely fine-grained and well dispersed, separation results can be unsatisfactory.

When the target macerals are not very abundant and more than milligram to gram quantities are needed, semicontinuous centrifugation can be used. This technique has been well described [12-13] and allows kilograms of sample to be processed per day. Because it operates at only a single density per run, sequential runs are necessary to concentrate a target maceral.

#### DISCRIMINATING SAMPLE SELECTION

The techniques described above will usually achieve successful separations on most coals, however, much higher yields and much shorter processing times are possible, if there are no constraints on the choice of the original sample, *i.e.* the target maceral is specified and not its source [14-16]. While most coals are composed of 50 to 90% vitrinite as shown in the density profile in Figure 1, some coals particularly the Permian Gondwana coals of the southern hemisphere are dominated by inertinite macerals. The density profile of such a coal from South Africa is as shown in Figure 2. It has an inertinite content of over 70% and is clearly an excellent choice for inertinite maceral separation. Other humic coals have higher than normal contents of specific macerals, such as the resinite rich coals from the western U.S. (see Figure 3). Sapropelic coals are dominated by sporinite (cannel coal), alginite (boghead coal) and bituminite, and thus make good candidates for the separation of these macerals. Although these coal types are not abundant, they are ubiquitous. The density profiles of a typical boghead coal along with two different cannel coals are given in Figures 4, 5, and 6 respectively. When appropriate whole coals cannot be found, selected layers in particular coal seams can sometimes be used. The layers, called lithotypes, are specific associations of macerals that can be quite different from the average composition of the whole coal seam. A common lithotype is the easiest to collect is fusain. It is composed of inertinite macerals, mainly semifusinite and fusinite. An example is shown in Figure 7. The two main peaks are natural concentrations of semifusinite (lower density) and fusinite (higher density). The vitrain lithotype is a natural concentration of vitrinite. It can be hand-picked with only moderate effort. As shown in Figure 8, it gives a density profile that shows only vitrinite. Figure 9 shows a monomaceralic boghead coal that shows only alginite.

#### REFERENCES CITED

1. Dyrkacz, G.; Bloomquist, C.; Horwitz, P.; Sep. Sci and Tech. 1981, **16**, No. 10, 1571
2. Dyrkacz, G.; Horwitz, P.; Fuel 1982, **61**, 3
3. Dyrkacz, G.; Bloomquist, C.; Ruscic, L.; Horwitz, P.; in "Chemistry and Characterization of Coal Macerals"; Winans, R. and Crelling J., Eds.; ACS Symp Ser. 252: Washington D.C., 1984, 65
4. Dyrkacz, G.; Bloomquist, C.; Ruscic, L.; Fuel 1984, **63**, 1166
5. Dyrkacz, G.; Bloomquist, C.; Solomon, P.; Fuel 1984, **63**, 536
6. King, H.; Dyrkacz, G.; Winans, R.; Fuel 1984, **63**, 341
7. Karas, J.; Pugmire, R.; Woolfenden, W.; Grant, D.; Blair, S.; Int. Jour. Coal Geol. 1985, **5**, 315
8. Crelling, J.; Ironmaking Proc. A.I.M.E., 1988, **47**, 351.
9. Crelling, J.; Proc. Inter. Conf. Coal Sci. -IEA, in Coal Science and Technology II, Elsevier, Amsterdam: 1987, 119
10. Crelling, J.; Skorupska, N.; Marsh, H.; Fuel 1988, **67**, 781
11. Crelling, J.; Pugmire, R.; Meuzelaar, H.; McClenen, H.; Karas, J.; Energy and Fuels, **5**, 668
12. Dyrkacz, G. R. and Bloomquist, C. A. A.; Energy and Fuels 1992, **6**, 374
13. Dyrkacz, Gary R.; Bloomquist, C. A. A.; and Ruscic, Ljiljana; Energy and Fuels 1992, **6**, 357
14. Skorupska, N.M.; Sanyal, A.; Hesselman, G. J.; Crelling, J.C., Edwards, I. A. S.; and Marsh, H.; Proc. Inter. Conf. Coal Sci.-IEA, in Coal Science and Technology II, Elsevier, Amsterdam: 1987, 119.
15. Crelling, John C.; Hippo, Edwin J.; Woerner, Bruce A.; and West Jr., David P.; Fuel, 1992, **71**, 151
16. Crelling, John C.; Thomas, K. Mark; and Marsh, Harry; Fuel, 1993, **72**, 339

**DENSITY PROFILE**  
Typical Humic Coal

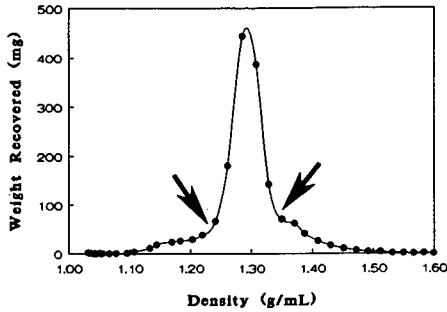


Figure 1. A typical density profile of an humic coal. The main peak represents the vitrinite group macerals, the low density shoulder represents the liptinite group, and the high density shoulder represents the inertinite group. The arrows indicate typical cut-points between the macerals groups.

**DENSITY PROFILE**  
Gondwana Coal

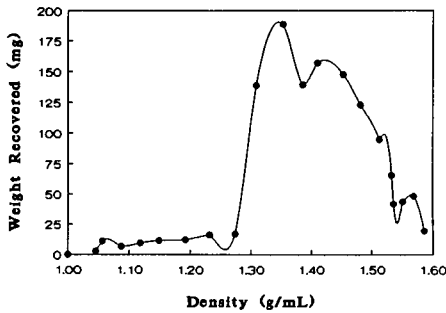


Figure 2. A typical density profile of an inertinite rich Gondwana coal. While the highest peak represents vitrinite the bulk of the sample is inertinite group macerals on the high density side of the vitrinite.

**DENSITY PROFILE**  
Resinite Rich Coal

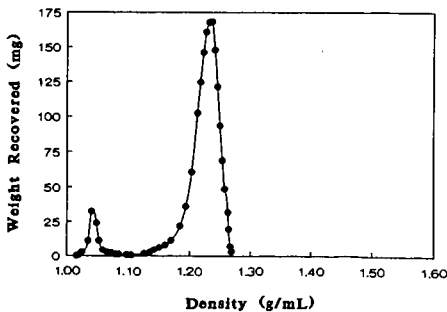


Figure 3. A density profile of a resinite rich coal from the western U.S. The major peak is the vitrinite maceral group, but the smaller very low density peak is resinite.

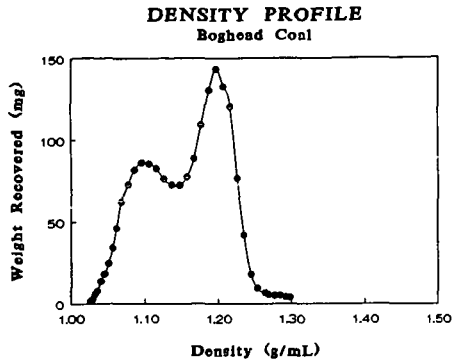


Figure 4. A density profile of a boghead coal. The main peak represents the amorphous kerogen (bituminite?) matrix and the well defined low density peak is alginite.

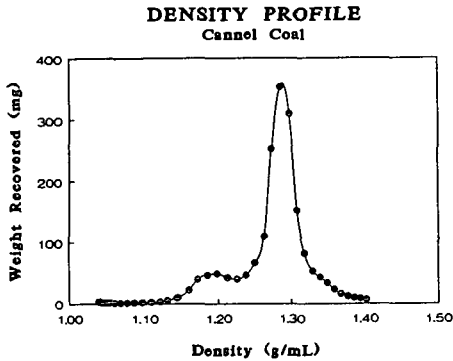


Figure 5. A density profile of a cannel coal. The main peak is vitrinite and the low density peak is sporinite.

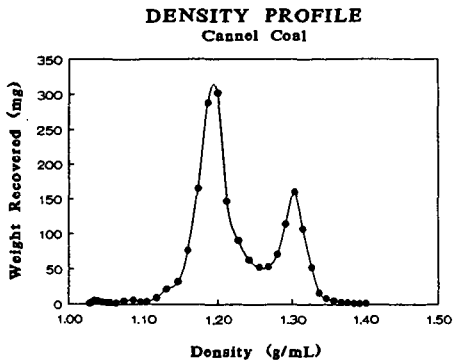


Figure 6. A density profile of another cannel coal which is extremely sporinite rich. In this case the dominant peak is sporinite and the smaller peak is vitrinite.

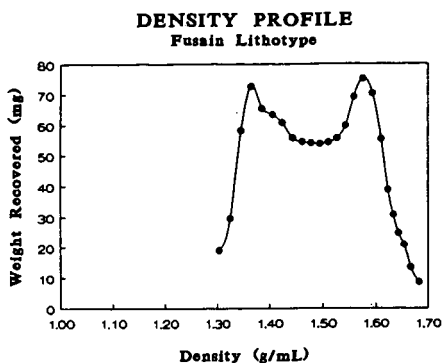


Figure 7. A density profile of a fusain lithotype. Note that it contains only inertinite macerals. The two peaks represent semifusinite (lower density) and fusinite (higher density).

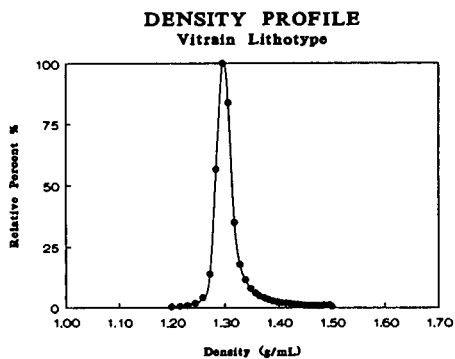


Figure 8. A density profile of a vitrain lithotype consisting of vitrinite and very little else.

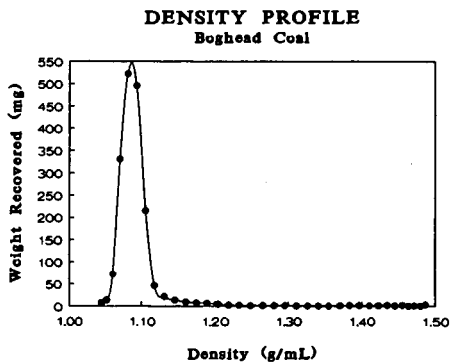


Figure 9. A density profile of a boghead coal that is essentially momomaceralic consisting of alginite.

## Adventures in Maceral Separation

Gary R. Dyrkacz  
Chemistry Division,  
Argonne National Laboratory  
9700 S. Cass Ave  
Argonne, Illinois 60439

### Introduction

Understanding coal structure tasks the best researchers with the latest equipment. The problems start with the raw materials to produce coal - the profusion of plant tissues and minerals of the peat swamps. The problems are further compounded by environmental processing of this raw material through a host of biochemical, chemical and thermal transformations.<sup>1</sup> The resulting coal is then physically and chemically heterogeneous, both in terms of the organic material and the mineral components. Just how heterogeneous is not even clear. Indeed, from the organic chemistry perspective, it is not even known whether any regular structure can even be assigned to coal.

Physically we divide coal into macroscopic or microscopic components called macerals as one measure of the physical heterogeneity. Some macerals are relatively easily associated with certain living tissues such as spores or algae. More often the identity of the original material is uncertain. Partly this is due to the accepted methods of preparing samples for microscopic observation, but often the original peat is so extensively degraded that any remnants of the original physical structure are gone.<sup>2</sup>

Because macerals are the first level of heterogeneity that can be readily observed, separating them to obtain more pure species would appear to be worthwhile. This is true even for a single maceral type, such as vitrinite, which can still be heterogeneous. However, it is notable that maceral separations are not routinely done, even when fundamental structure studies are anticipated. This is contrary to many other fields (e.g. plant science or bioscience areas) where physical and chemical separations of complex organic materials is a mandatory first stage in unraveling structures. One reason may have been a lack of maceral separation science. One of our goals has been to put maceral and, lately, submaceral separations on a more scientific basis.

The methodology of maceral separations can be broken down into several processes which are listed in Table 1. Each of these processes, when viewed in depth, is intertwined with complex and often little understood issues of coal's physical and chemical structure. As a result viable separation procedures are achieved mostly by guessing, faith and a lot of work. For efficient maceral separations to be realized, all these subprocesses must interlock in concert. We have been able to either thread our way through or skirt a number of the problems. However, there is still a largely unexplored vein of information within each area that is specifically important to maceral separations, and probably generally to coal science. A complete idea of where work is needed to improve separations cannot be fully addressed here. Only a brief overview and flavor of where work stands can be given.

### Discussion

#### *Liberation*

Coal constituents must be liberated from each other for optimal separation even to be possible. Without sufficient liberation some macerals may not be liberated at all. At best, they can only be enriched. Incomplete liberation also affects other constituents by limiting the pure materials that can be separated. This can potentially bias the type of material that is recovered as monomaceral particles. For example, lipinites are usually difficult to liberate cleanly from vitrinites. In density separations, these bimaceral particles will usually be found mixed in with low density monomaceral vitrinite particles. This vitrinite is different from any of the other vitrinite material.<sup>3</sup> Eliminating this portion of material to obtain pure vitrinite can lead to differences in vitrinite properties that do not reflect the original coal.

Mechanical grinding has been the primary method for liberation. The small size of many maceral species means that the coal must be ground very fine - on the order of 10 microns. Fluid energy

mills appear to be particularly effective at producing coal particles in this range. They also appear to cause the least amount of reaccrion or rehomogenization of the coal.<sup>4</sup>

What is the appropriate stage to stop grinding? This question is not only important from the aspect of maceral separation, but can extend to how we perceive the chemical heterogeneity of coal. Ideally, grinding needs to be continued until all particles are completely monomaceral. This goal is opposed by the problem of identification of the ground material. Simple optical identification based on reflectance differences between the macerals is not possible below about 2 microns. In addition, another limiting factor is reached in the submicron range (<0.5 microns). Particles in this range can strongly interact with separation media giving quite different densities than larger particles with the same density.<sup>5</sup>

The preceding demands of maceral liberation critically depend on the maceral concept and maceral identification. But what is the nature of chemical heterogeneity within even a single monomaceral particle? If coal is ground to submicron sizes will new distinct particulate species appear? This would suggest that macerals themselves consist of chemical domains of regular structure? Often vitrinite will exhibit detailed substructures, when coal samples are polished and etched.<sup>1,2</sup> Alternatively, what if no further resolution occurs? This would be true if coal is so heterogeneous that its structure varies on a nanometer scale, or if monomaceral particles are chemically homogeneous. These questions are not easy to answer, but point to a level of physical separation that has received only a small amount of attention.<sup>4</sup>

#### ***Demineralization***

The common minerals found in coal have densities from ~1.5 to 4 times that of the organic coal material. Thus, a small amount of included mineral can have a large influence on maceral particle density. Optimum separation of macerals demands that the coal be as mineral free as possible. Mechanical demineralization by density methods is not sufficient to remove the inorganic materials.<sup>3</sup> Chemical demineralization using strong acids is the alternative, but the effect of this procedure on the chemical structure of coal is still uncertain. Fortuitously, pyrite, which has a density of ~4.5 g cm<sup>-3</sup> and is particularly difficult to remove chemically, is nearly completely liberated from the coal particles during fluid energy mill grinding.

#### ***Wetting and Dispersion***

Most maceral separations are based on differences in maceral densities in liquid suspensions. If coal particles extensively aggregate in a medium, then separation will be inefficient. There are two related components to the problem: 1. The coal particles must be completely wetted by the media. 2. The particles must remain isolated from one another or undergo nearly elastic collisions over the separation time. Wetting is a necessary condition for dispersion. Just what governs the effectiveness of a particular media for maceral particle dispersion is not clear. The result is that the dispersion remains in the realm of "shake-the-shelf" chemistry. An example of the importance of dispersion can be seen in Figure 1. This data is taken from a study of centrifugal sink/float separations for coal in a variety of commonly used suspension media.<sup>6</sup> SI is a separation index, which is a measure of the efficiency of separation. An SI value of 0 represents no separation relative to the original coal while 1 represents a complete disengagement of the float and sink material. A negative value is due to aggregation effects. RI is the recovery index and represents the fraction of float or sink phase found after separation, relative to the maximum fraction of material expected from a perfect separation. Thus, a value of 0 represents no desired phase found, while 1 represents all the phase isolated. Of the five media systems investigated, only two stood out: aqueous CsCl/Brij-35 and Ca(NO<sub>3</sub>)<sub>2</sub>/Brij-35. (Brij-35 is the nonionic surfactant polyoxyethylene-23-lauryl ether.) Other commonly used media, such as ZnCl<sub>2</sub> or organic systems based on CCl<sub>4</sub>, were not as effective. Contrary to expectations, recycling material in aggregating media showed no further separation. Although Brij-35 seems to be a magic material that fixes all dispersion problems, it is not. Separations in aqueous ZnCl<sub>2</sub>/Brij-35 solutions were only moderately better than ZnCl<sub>2</sub> solutions. Thus, the effect of the media can be subtle. Much more work is needed to understand what drives the interactions.

#### ***Separation***

The heart of maceral enrichment is the separation step. Sedimentation methods are the most commonly used, particularly centrifugal sink/float. A relative newcomer on the maceral separation scene is density gradient centrifugation(DGC). This technique is superior to any type of sink/float separation. It has the highest density resolving ability of any maceral separation method, and

functions both as a separation and characterization method. DGC methods are definitely the method of choice for optimum enrichment of macerals. However, DGC methods do have limitations on the amount of material than can be obtained in any single separation cycle. This can be overcome by first using sink/float methods to isolate desired density regions.

In some studies high density resolution of macerals may not be necessary. Thus, sink/float techniques will remain an alternate separation method or at least an adjunct to DGC separations. With this in mind, we have recently examined the process of centrifugal sink/float (S/F) separations to understand its limitations and provide guidance in its use.<sup>5,7</sup> In addition, we have explored in detail a continuous flow centrifugation (CFC) technique that allows much larger amounts of material to be separated in a shorter time than by simple centrifugal sink/float.<sup>8-10</sup> Both studies could not have been done without the resolving power and speed of analytical density gradient centrifugation (ADGC) methods. Each study required over two hundred separate ADGC analyses of float or sink phases.

Several general observations emerged from the sink/float studies. The effect of media has already been discussed. Figure 2 displays the ADGC results of a complete separation sequence on a single high volatile bituminous coal using CsCl/Brij-35. The vertical bars represent the nominal solution densities used for each fractionation. This particular separation sequence was from low density to high density. Note that several fractions are not very pure. This is a consequence of two effects. First, even though a density separation may have a constant separation efficiency (i.e., the fraction of mass that will report to the proper phase), the amount of contamination depends on the efficiency factor and the density distribution. Hence, separations made near large bands will be more contaminated than separations further from the main band. We were able to predict the purity of fractions based on the former effect with only moderate success. The second general observation is that float phases invariably contaminates the sink phase due to solution instabilities during the centrifugation process. Much more work is needed to optimize and predict the dynamics of such separations. In the course of this work, we also realized that the density interval of a fraction can also dramatically effect the purity. The narrower the density interval between successive separations, the more contaminated will be the resulting fractions. This is due to the fact that the separation inefficiency is constant, but the mass of a fraction will be smaller as the density interval between separations decreases. DGC is not as affected by this phenomena; this is one reason for its high resolving power. Generally, the S/F separations produced fractions with purities >60 %. Many fractions were routinely better than 80% pure.

Continuous flow centrifugation separations, another version of sink/float separations, had very similar constraints to the simple centrifugal sink/float. Even the overall fraction purities were about the same. CFC separations are carried out in a special centrifuge that allows the continuous removal of liquid from the rotor. Float material is entrained with the expelled liquid, while sink material is retained in the rotor (or in more sophisticated centrifuges, separately ejected). Very dilute solutions can be used so that particle aggregation can be minimized. Single density separations with up to 300g of coal can be accomplished within a day. This is far more than can be conveniently handled by simple centrifugal sink/float methods for finely ground coal. We believe that the efficiency of CFC separations can be substantially improved. For one the rotor dynamics appeared to be more complicated than generally believed. We suspect that there are regions within the separation section of the rotor where the particles are not subjected to the expected flow and centrifugal dynamics. Detailed studies of this device are needed to corroborate this. Modifications to the rotor may be necessary to increase the efficiency.

### **Isolation**

Isolation is included in Table 1 mainly because of its impact on time for a complete separation cycle. The largest fraction of time in the separation of ultrafine coal is spent filtering and washing the separated samples. It is often wise to use membrane filters to avoid selective loss of fine coal, which further slows the filtration process.

### **Summary**

Progress has been made in recent years in the science of maceral separation. However, there are many areas that can improved, and new areas to be investigated. The power of DGC to physically resolve macerals and submaceral species coupled with other instrumental techniques is particularly attractive for defining the limits of coal heterogeneity as well as investigating the ability of other separation methods.

## Acknowledgement

This work was performed under the auspices of the Office of Basic Energy Sciences, Division of Chemical Sciences, U. S. Department of Energy, under contract number W-31-109-ENG-38.

## References

1. Stach, E., Mackowsky, M.-Th., Teichmuller, M., Taylor, G. H., Chandra, D., Teichmuller, R., Murchinson, D.G., and Zienke, F., 'Stach's Textbook of Coal Petrology', 2nd Edn., Gebruder Borntraeger, Berlin, 1975.
2. Kroger, C., *Erdol und Kohle Erdgas Petrochem.*, 1964, 17, 802-812.
3. Dyrkacz, G. R., Bloomquist, C. A. A., and Ruscic, L. R., *Fuel*, 1984, 63, 1166-1173.
4. Dyrkacz, G. R., Bloomquist, C. A. A., in preparation.
5. Dyrkacz, G. R., and Horwitz, E. P., *Fuel*, 1982, 61, 3-12.
6. Dyrkacz, G. R., Ruscic, L.R., and Fredericks, J., *Energy and Fuels*, 1992, 6, 720-742.
7. Dyrkacz, G. R., Ruscic, L.R., *ibid.*, 1992, 6, 743-752.
8. Dyrkacz, G. R., Bloomquist, C. A. A., *ibid.*, 1992, 6, 357-374.
9. Dyrkacz, G. R., Bloomquist, C. A. A., *ibid.*, 1992, 6, 375-386.
10. Dyrkacz, G. R., Bloomquist, C. A. A., Ruscic, L.R., *ibid.*, 1992, 7, 655-660.

**Table 1. Coal Maceral Separation Subprocesses.**

---

Liberation of constituents  
 Demineralization  
 Wetting and dispersion of maceral particles  
 Separation  
 Isolation

---

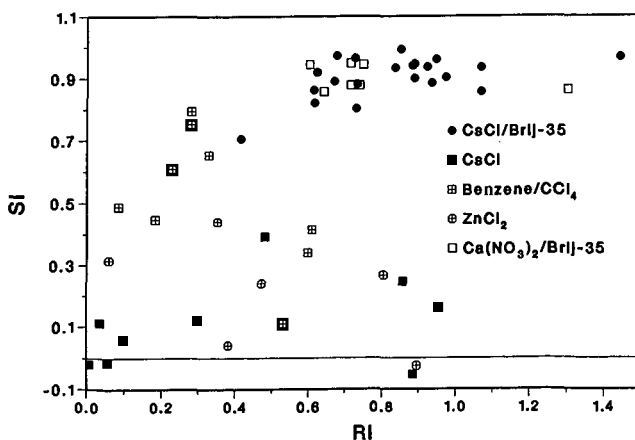


**Figure 1.** S/F Separation and recovery indices for float fractions from three high volatile bituminous coal.

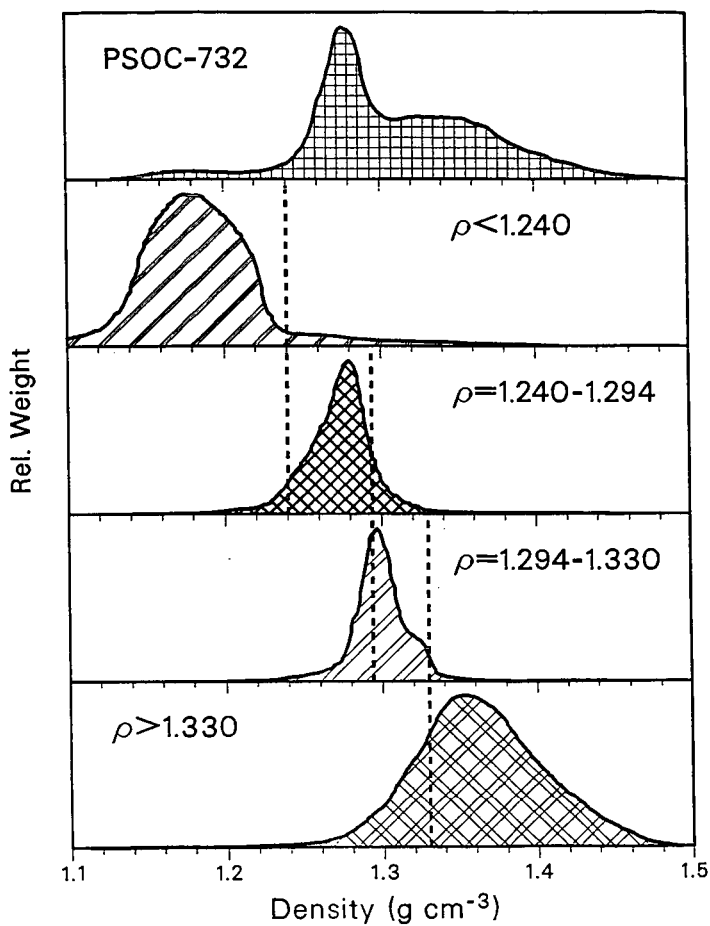


**Figure 2.** Sequential S/F Separation of a high volatile bituminous coal distributions are normalized to peak values.